**Atmospheric
Chemistry
and Physics**

Rate coefficients for the gas-phase reaction of OH with (Z)-3-hexen-1-ol, 1-penten-3-ol, (E)-2-penten-1-ol, and (E)-2-hexen-1-ol between 243 and 404 K

M. E. Davis[1,2,*] and J. B. Burkholder[1]

[1]Earth System Research Laboratory, Chemical Sciences Division, NOAA, 325 Broadway, Boulder
Colorado 80305-3328, USA
[2]Cooperative Institute for Research in Environmental Sciences, University of Colorado, Boulder 80309, USA
[*]current address: Michigan State University, East Lansing, MI 48825, USA

Abstract. Rate coefficients, k, for the gas-phase reaction of the OH radical with (Z)-3-hexen-1-ol ((Z)-$CH_3CH_2CH=CHCH_2CH_2OH$) (k_1), 1-penten-3-ol ($CH_3CH_2CH(OH)CH=CH_2$) (k_2), (E)-2-penten-1-ol ((E)-$CH_3CH_2CH=CHCH_2OH$) (k_3), and (E)-2-hexen-1-ol ((E)-$CH_3CH_2CH_2CH=CHCH_2OH$) (k_4), unsaturated alcohols that are emitted into the atmosphere following vegetation wounding, are reported. Rate coefficients were measured under pseudo-first-order conditions in OH over the temperature range 243–404 K at pressures between 20 and 100 Torr (He) using pulsed laser photolysis (PLP) to produce OH radicals and laser induced fluorescence (LIF) to monitor the OH temporal profile. The obtained rate coefficients were independent of pressure with negative temperature dependences that are well described by the Arrhenius expressions

$$k_1(T) = (1.3 \pm 0.1) \times 10^{-11} \exp[(580 \pm 10)/T];$$
$$k_1(297\,\mathrm{K}) = (1.06 \pm 0.12) \times 10^{-10}$$

$$k_2(T) = (6.8 \pm 0.7) \times 10^{-12} \exp[(690 \pm 20)/T];$$
$$k_2(297\,\mathrm{K}) = (7.12 \pm 0.73) \times 10^{-11}$$

$$k_3(T) = (6.8 \pm 0.8) \times 10^{-12} \exp[(680 \pm 20)/T];$$
$$k_3(297\,\mathrm{K}) = (6.76 \pm 0.70) \times 10^{-11}$$

$$k_4(T) = (5.4 \pm 0.6) \times 10^{-12} \exp[(690 \pm 20)/T];$$
$$k_4(297\,\mathrm{K}) = (6.15 \pm 0.75) \times 10^{-11}$$

(in units of $\mathrm{cm^3\,molecule^{-1}\,s^{-1}}$). The quoted uncertainties are at the 2σ (95% confidence) level and include estimated systematic errors. The rate coefficients obtained in this study are compared with literature values where possible.

1 Introduction

Biogenic volatile organic compounds (BVOCs) are emitted into the atmosphere in quantities that exceed the emission of VOCs from anthropogenic sources (Guenther et al., 2000, 1995). BVOCs are chemically active compounds and their gas-phase chemistry has a direct impact on air quality on local to regional scales through their impact on the abundance of HO_x ($HO_x = OH + HO_2$), ozone production, and contributions to secondary organic aerosol (SOA). The formation of organic nitrates locally also leads to the transport of NO_x ($NO_x = NO + NO_2$) and subsequent ozone production on the regional and continental scale. It is therefore important to know not only the atmospheric abundance of BVOCs, but also their reaction rates and degradation pathways to enable accurate model calculations used for air quality forecasts as well as regulatory purposes.

A number of unsaturated BVOCs (molecules containing carbon-carbon double bonds) are emitted by a variety of plant species in response to wounding due to their antibacterial properties (Nakamura and Hatanaka, 2002). The unsaturated compounds primarily include C5 and C6 aldehydes, ketones, and alcohols and are collectively referred to as "green leaf volatiles". The atmospheric lifetimes of these oxygenated BVOCs and the formation of atmospheric degradation products from these compounds are greatly influenced by the presence of the $>C=C<$ double bond, to
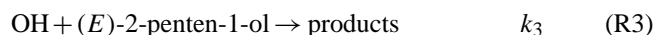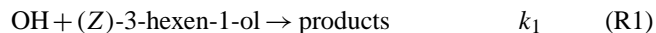
Correspondence to: J. Burkholder
(james.b.burkholder@noaa.gov)

which radicals such as OH, O_3, and NO_3 can add, and the presence of functional groups. (Z)-3-hexen-1-ol ((Z)-$CH_3CH_2CH = CHCH_2CH_2OH$), leaf alcohol, is emitted into the atmosphere following the enzymatic oxidation of α-linolenic acid in response to stress, e.g. drought, (Ebel et al., 1995) and vegetation wounding (Hatanaka and Harada, 1973). (Z)-3-hexen-1-ol is emitted globally from a wide range of plants including grass, clover, alfalfa, grape, lettuce, onion, orange, peach, and oak (Arey et al., 1991; Kirstine et al., 1998). Another significant C6 green leaf volatile associated with the wounding of plants is (E)-2-hexen-1-ol ((E)-$CH_3CH_2CH_2CH = CHCH_2OH$) (Kirstine et al., 1998). Several C5 oxygenates derived from α-linolenic acid are also emitted by vegetation for the purpose of microbiological protection. These compounds include 1-penten-3-ol ($CH_3CH_2CH(OH)CH = CH_2$) and 2-penten-1-ol ($CH_3CH_2CH = CHCH_2OH$) which are emitted by a variety of plants (Fisher et al., 2003; Heiden et al., 2003; Karl et al., 2001; Kirstine et al., 1998).

Green leaf unsaturated alcohols are primarily removed from the atmosphere by reaction with the OH radical (Alvarado et al., 1999; Aschmann et al., 1997; Atkinson et al., 1995; Baasandorj and Stevens, 2007; Baker et al., 2004; Orlando et al., 2001; Papagni et al., 2001; Upadhyaya et al., 2001), NO_3 (Noda et al., 2000, 2002; Pfrang et al., 2006, 2007), and O_3 (Alvarado et al., 1999; Aschmann et al., 1997; Atkinson et al., 1995; Grosjean and Grosjean, 1997) leading to the formation of oxygenated degradation products. An atmospheric lifetime for (Z)-3-hexen-1-ol of several hours under typical tropospheric conditions has been estimated based on its gas-phase reaction with OH, NO_3, and O_3 (Atkinson et al., 1995).

In this study, gas-phase rate coefficients for the reaction of four atmospherically relevant unsaturated alcohols with the OH radical

$$OH + (Z)\text{-3-hexen-1-ol} \rightarrow \text{products} \qquad k_1 \qquad (R1)$$

$$OH + 1\text{-penten-3-ol} \rightarrow \text{products} \qquad k_2 \qquad (R2)$$

$$OH + (E)\text{-2-penten-1-ol} \rightarrow \text{products} \qquad k_3 \qquad (R3)$$

$$OH + (E)\text{-2-hexen-1-ol} \rightarrow \text{products} \qquad k_4 \qquad (R4)$$

were measured over a range of temperature (243–404 K) and pressure (20–100 Torr, He). This work is a continuation of a previous study from this laboratory in which temperature dependent rate coefficients for the reaction of OH with several green leaf unsaturated aldehydes were reported (Davis et al., 2007). Previous studies have reported room temperature reaction rate coefficients for Reactions (R1) (Atkinson et al., 1995) and (R2) (Orlando et al., 2001). During the course of this work another kinetic study of Reactions (R1) and (R2) was reported (Jiménez et al., 2009). We have compared our results with these previous studies and the rate coefficient for

the analogous well studied OH + $(CH_3)_2C(OH)CH = CH_2$ (2-methyl-3-buten-2-ol, MBO) reaction. We also briefly examine the reactivity trends for the (E)- and (Z)- isomers.

2 Experimental details

Rate coefficients for Reactions (R1)–(R4) were measured under pseudo-first-order conditions in the OH radical, [Alcohol] $\gg$ [OH], using pulsed laser photolysis (PLP) to produce OH radicals and laser induced fluorescence (LIF) to measure OH radical temporal profiles. A schematic of the experimental apparatus is shown in Fig. 1. The PLP-LIF apparatus has been used extensively in our laboratory and is described in detail elsewhere (Davis et al., 2007; Vaghjiani and Ravishankara, 1989). A particular emphasis in this work was placed on the accurate determination of the reactant concentration in the LIF reactor by using on-line spectroscopic measurements and precise gas flow measurements. A description of the experimental methods used and a brief description of the experimental apparatus are given below.

2.1 Experimental apparatus

Rate coefficients were measured in a $150\,cm^3$ jacketed 15 cm long Pyrex LIF reactor. The temperature of the reactor was maintained by circulating fluid from a heating (or cooling) reservoir through its jacket. The temperature of the gas in the reaction zone of the reactor was measured using a calibrated retractable thermocouple to within $\pm 1\,K$.

OH radicals were produced by pulsed laser photolysis of H_2O_2 or HNO_3 at 248 nm (KrF excimer laser) or HONO (DONO) at 351 nm (XeF excimer laser). DONO photolysis was used to produce OD radicals. The initial OH radical concentration, $(OH)_0$ (molecule cm^{-3}), was estimated from the precursor concentration, its absorption cross section, $\sigma(\lambda)$ (cm^2 molecule^{-1}), and quantum yield, $\Phi(\lambda)$, at the photolysis wavelength, λ, and the photolysis laser fluence, F (photons mJ^{-1} pulse^{-1})

$$[OH]_0 = \sigma(\lambda)\Phi(\lambda)F[\text{precursor}] \qquad (1)$$

The photolysis laser fluence was measured at the exit of the LIF reactor using a calibrated power meter and fluences in the range 1–16 mJ cm^{-2} pulse^{-1} (1.25×10^{15} photons mJ^{-1} at 248 nm and 1.76×10^{15} photons mJ^{-1} at 351 nm) were used. The OH precursor concentration was estimated from the measured OH decay in the absence of the alcohol reactant and the rate coefficient for the reaction of the precursor with OH (Sander et al., 2006). The precursor concentration varied in the range $(0.4–3.0) \times 10^{14}$ molecule cm^{-3} (H_2O_2), $(0.3–2.8) \times 10^{15}$ molecule cm^{-3} (HNO_3), and $(0.4–1.6) \times 10^{14}$ molecule cm^{-3} (HONO). The initial OH radical concentration was in the range $(0.6–4.7) \times 10^{11}$ molecule cm^{-3}. Using low initial OH radical concentrations minimized second order radical-radical chemistry on the time scale of our OH
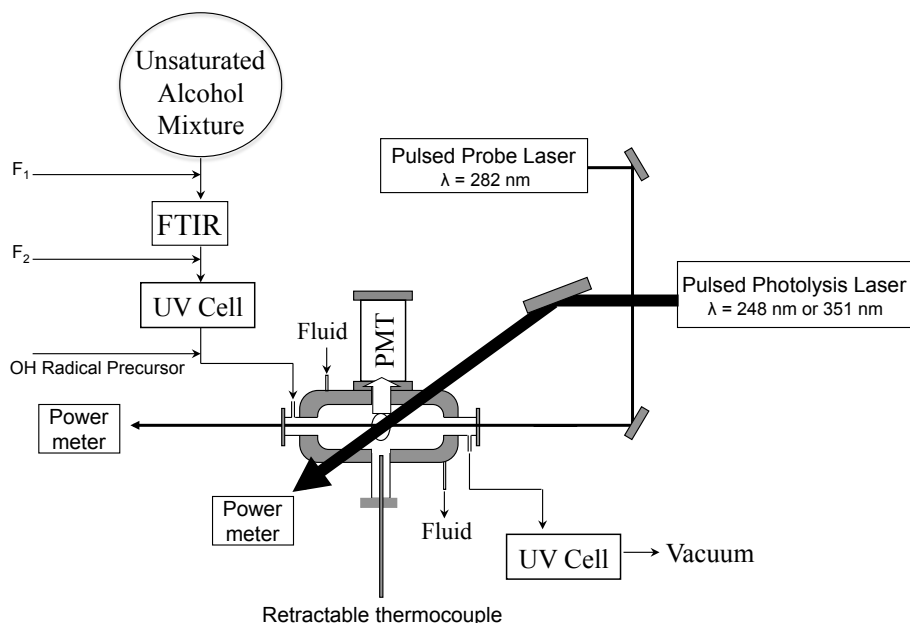
Fig. 1. Schematic of the pulse laser photolysis-laser induced fluorescence (PLP-LIF) apparatus. F_1 and F_2 indicate bath gas flows.

profile measurements. H_2O_2 was used as the OH radical precursor in the majority of the experiments, while HNO_3 and HONO were used in several experiments to evaluate possible systematic errors in the rate coefficient measurements.

The OH radical was excited in the $A\,^2\Sigma^+\,(v'=1) \leftarrow X\,^2\Pi$ $(v''=0)$ band near 282 nm (OD was excited near 287 nm) using the frequency-doubled output of a pulsed Nd:YAG pumped dye laser. The OH fluorescence signal was detected by a photomultiplier tube (PMT) mounted orthogonal to the photolysis and probe laser beams. A band-pass filter (peak transmission at 310 nm with a 20 nm band-pass, FWHM) mounted in front of the PMT was used to isolate the OH fluorescence signal. The PMT signal was averaged for 100 laser shots using a gated charge integrator. OH temporal profiles were obtained by varying the delay between the photolysis and probe lasers, the reaction time, between 10 μs and 50 ms.

OH temporal profiles were measured under pseudo-first-order conditions in OH and the OH decay obeyed the relationship

$$\ln\left(\frac{[\text{OH}]_t}{[\text{OH}]_0}\right) = \ln\left(\frac{S_t}{S_0}\right) = -(k_i[\text{Alcohol}] + k_d)\,t = -k't \quad (2)$$

where S_t is the OH LIF signal at time t that is proportional to $[\text{OH}]_t$, k' and k_d are the pseudo-first-order rate coefficients measured in the presence and absence of the alcohol reactant. k_d represents the loss of OH radicals due to a combination of reaction with the OH precursor and buffer gas impurities and diffusion out of the detection volume. Values of k_d were between 50 and $200\,\text{s}^{-1}$. k' was measured for a range of [Alcohol] at each temperature and $k_i(T)$ was determined from the slope of k' versus [Alcohol].

2.2 Alcohol concentration determination

The concentration of (Z)-3-hexen-1-ol, 1-penten-3-ol, (E)-2-penten-1-ol, or (E)-2-hexen-1-ol in the LIF reactor was determined by on-line UV and infrared absorption measurements as well as measured flow rates of the sample from dilute gas mixtures. UV (185 nm) and infrared absorption cross sections were measured as part of this study using the Beer-Lambert law

$$A = -\ln\left(\frac{I}{I_0}\right) = \sigma(\lambda)\,L\,[\text{Alcohol}] \quad (3)$$

where L is the pathlength of the absorption cell and the alcohol concentration was determined by absolute pressure measurements.

UV absorption of the alcohols was determined using a Hg pen-ray lamp light source combined with a solar-blind photodiode detector with a 185 nm band-pass filter. A similar setup was used for the cross section determination and in the kinetic measurements. For the cross section measurements, two absorption cells with quartz windows and optical pathlengths of 1.0 and 1.95 cm were used. The absorption cells used for monitoring the concentration in the LIF reactor during the kinetic measurements had 50 cm pathlengths. I_0 was measured with the absorption cell flushed with bath gas (He) or evacuated. A flow of the pure alcohol vapor was then introduced and the lamp intensity, I, as well as the absolute pressure recorded. The pressure of the alcohol in the absorption cell varied over the range 0.1–0.6 Torr (the exact pressure range differed depending on the molecule) to obtain the absorption cross section using Eq. (3).

Table 1. Summary of UV and infrared absorption cross sections for (Z)-3-hexen-1-ol, 1-penten-3-ol, (E)-2-penten-1-ol, and (E)-2-hexen-1-ol measured in this work and taken from the literature.

Compound	UV Cross Sections			Infrared Cross Sections[b]		
	σ (185 nm)[a] (10^{-17} cm^2 molecule^{-1})	Reference	Peak position (cm^{-1})	Peak cross section (10^{-20} cm^2 molecule^{-1})	Band strength[c] (10^{-17} cm^2 molecule^{-1} cm^{-1})	
(Z)-3-hexen-1-ol	3.26±0.16	This work	2973.3	44.8	3.80±0.20	
	4.04±1.50	Jimenez et al. (2009)				
1-penten-3-ol	1.42±0.08	This work	2971.8	38.1	2.54±0.13	
	1.28±0.42	Jimenez et al. (2009)				
(E)-2-penten-1-ol	1.90±0.10	This work	2972.3	29.4	2.70±0.14	
(E)-2-hexen-1-ol	1.74±0.09	This Work	2969.4	24.0	2.08±0.11	

[a] Quoted uncertainties are 2σ including estimated systematic errors, the precision of the cross section measurements from this work was ±(1−2)%.
[b] Infrared absorption spectra between 800–4000 cm^{-1} are given in the supporting information.
[c] Integration interval was 2800–3050 cm^{-1}.

Infrared cross sections were obtained relative to the UV absorption cross section at 185 nm as follows. A slow gas flow of a dilute alcohol/He mixture was passed through a UV absorption cell (50 cm) and then through an infrared absorption cell. Infrared absorption measurements were made using a Fourier transform infrared spectrometer (FTIR) with 100 co-added scans at a resolution of 1 cm^{-1}. A single pass infrared absorption cell with a pathlength of 10 cm was used for the majority of the measurements. A small volume (∼750 cm^3) multi-pass absorption cell with a total optical pathlength of 485 cm was used in a few measurements. Good agreement was obtained for the spectra obtained using the two absorption cells. The sample then passed through a second UV absorption cell after the infrared cell to test for sample loss; no loss was observed. The infrared absorption cross sections were determined using the concentrations determined from the UV absorption measurements and the pressures measured in the absorption cells. The UV and infrared absorption cross sections obtained in this work are given in Table 1. Figures showing the infrared absorption spectra are given in the Supporting Information.

It is important to note that in our methods the UV and infrared absorption cross sections were not measured independently and rely on the absolute pressure measurements used in the UV cross section determination and the preparation of the sample bulb mixtures. In our kinetic measurements, using a combination of UV and infrared measurements provided a self-consistency check of the alcohol concentration determination and also provided a means to evaluate the loss of reactant in the gas flow through the apparatus, which is a particularly important issue at the temperature extremes employed in this study.

2.3 Materials

(Z)-3-hexen-1-ol (>98%), 1-penten-3-ol (99%), (E)-2-penten-1-ol (95%), and (E)-2-hexen-1-ol (96%) samples were degassed in several freeze-pump-thaw cycles and stored under vacuum in Pyrex reservoirs with Teflon values. Calibrated dilute mixtures (<0.3%) of the low vapor pressure (Z)-3-hexen-1-ol, 1-penten-3-ol, (E)-2-penten-1-ol, and (E)-2-hexen-1-ol compounds in He were prepared manometrically in darkened 12 L Pyrex bulbs. Gas chromatography/mass spectrometry was used to analyze the vapor of the liquid alcohol samples; the vapor was used to prepare the alcohol/He mixtures for the kinetic measurements. No detectable impurities, estimated to be <50 ppb, were observed in the (Z)-3-hexen-1-ol, (E)-2-penten-1-ol, and (E)-2-hexen-1-ol samples. The 1-penten-3-ol sample contained small but detectable amounts of 2-pentanol and several ketones, estimated to be <1 ppm. The impurity levels of these compounds are sufficiently low so as not to interfere with the determination of k_2; the rate coefficient for the OH + 2-pentanol reaction is ∼1.2×10^{-11} cm^3 molecule^{-1} s^{-1} at 298 K.

For the kinetics measurements, the alcohol samples were introduced into the gas flow from dilute mixtures that were prepared off-line, as shown in Fig. 1. The gas flow of the dilute alcohol/He mixture was measured using a calibrated flow meter. The sample was diluted with a bath gas flow before entering the FTIR. The sample was diluted further prior to entering the first UV absorption cell. A flow of purge gas added in front of the windows of the LIF reactor led to a small, ∼1%, dilution to the alcohol concentration measured after the LIF reactor. The absolute alcohol concentration in the LIF reactor was also measured using calibrated measured flow rates and pressures as well as the on-line spectroscopic measurements described above. The three methods agreed very well, to within <3%, under all experimental conditions.

He (UHP, >99.9995%) and O$_2$ (UHP, >99.99%) were used as supplied. Concentrated H$_2$O$_2$ (>95% mole fraction) was prepared by bubbling N$_2$ for several days through a sample that was initially ∼60% mole fraction. The H$_2$O$_2$ concentration in solution was determined by titration with a standard KMnO$_4$ solution. HONO (DONO) was prepared on-line by dropwise addition of a 0.1 M NaNO$_2$ solution (in H$_2$O or D$_2$O) to 10% H$_2$SO$_4$ (D$_2$SO$_4$) in H$_2$O (D$_2$O). The OH precursor was added to the gas flow by bubbling He through the liquid. The OH radical precursor was added to the gas flow just prior to the flow entering the LIF reactor. Gas flows were measured using calibrated flow transducers and pressures were measured using calibrated 1, 100, and 1000 Torr capacitance manometers.

3 Results and discussion

Tables 2–5 summarize the experimental conditions used in the determination of k_1–k_4 and the measured rate coefficients. The kinetic measurements for (Z)-3-hexen-1-ol, 1-penten-3-ol, (E)-2-hexen-1-ol, and (E)-2-penten-1-ol exhibit very similar behavior and were found to be independent of pressure over the range 20–100 Torr (He). Figure 2 shows a set of OH temporal profiles that illustrate the precision of the measured pseudo-first-order decays and the dependence on the alcohol concentration. The OH decays shown in Fig. 2 are for the OH + 1-penten-3-ol reaction at 297 K but similar quality data was obtained for the other compounds as well as under other experimental conditions.

Figure 3 shows the pseudo-first-order rate coefficient data for the OH + (Z)-3-hexen-1-ol, OH + 1-penten-3-ol, OH + (E)-2-hexen-1-ol, and OH + (E)-2-penten-1-ol reactions obtained at 244, 297, and 374 K. The k' determinations were very precise at all temperatures and under all experimental conditions as outlined in Tables 2–5. The obtained rate coefficients were independent of the variations in experimental parameters such as laser fluence, radical source (H$_2$O$_2$, HNO$_3$, HONO), initial OH concentration, precursor concentration, flow velocity, and the presence of O$_2$ (discussed further below). The final rate coefficient at each temperature was obtained by fitting all available pseudo-first-order rate data together, Eq. (2).

As expected, Reactions (R1)–(R4) are all efficient, although differences in reactivity were observed within the high precision of our measurements. The greatest difference in the measured rate coefficients was between the (Z)- and (E)-isomers, which is discussed further below. The final room temperature rate coefficients are

$$k_1(297\,\text{K}) = (1.06 \pm 0.04) \times 10^{-10}\,\text{cm}^3\,\text{molecule}^{-1}\,\text{s}^{-1}$$
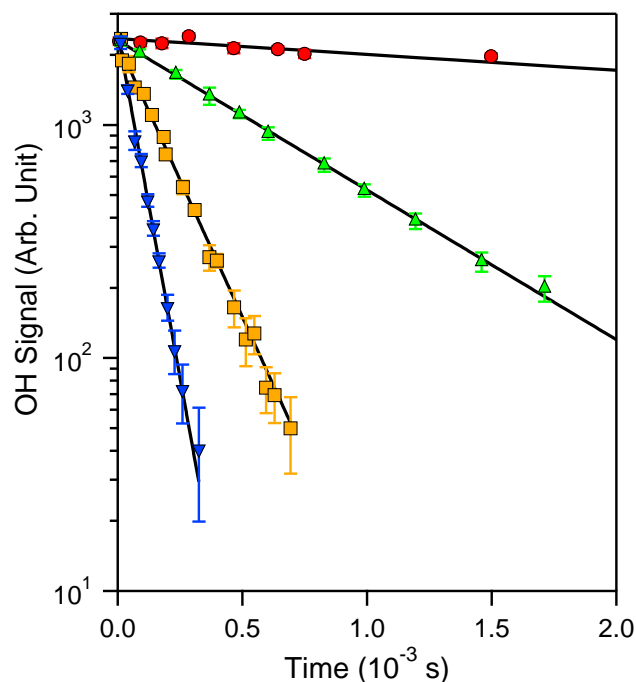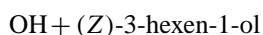
$$\text{OH} + (Z)\text{-3-hexen-1-ol}$$

Fig. 2. Representative OH radical pseudo-first-order decays measured for the reaction of OH with 1-penten-3-ol, k_2. Experimental conditions: 50 Torr (He) at 297 K, [OH]$_0$ = 1.4 × 10^{11} molecule cm^{-3}, photolysis laser fluence = 11 mJ cm^{-2} pulse^{-1} for 1-penten-3-ol concentrations of (in units of 10^{14} molecule cm^{-3}): 0 (○), 0.16 (△), 0.79 (□), and 1.9 (▽). The error bars are the 2σ precision error in the measured OH signal. The lines are the least-squares fits of the data to Eq. (2) where the slope yields k'.
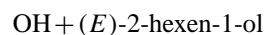
$$k_2(297\,\text{K}) = (7.12 \pm 0.14) \times 10^{-11}\,\text{cm}^3\,\text{molecule}^{-1}\,\text{s}^{-1}$$

$$\text{OH} + \text{1-penten-3-ol}$$
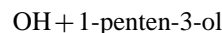
$$k_3(297\,\text{K}) = (6.76 \pm 0.17) \times 10^{-11}\,\text{cm}^3\,\text{molecule}^{-1}\,\text{s}^{-1}$$

$$\text{OH} + (E)\text{-2-penten-1-ol}$$
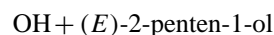
$$k_4(297\,\text{K}) = (6.15 \pm 0.43) \times 10^{-11}\,\text{cm}^3\,\text{molecule}^{-1}\,\text{s}^{-1}$$

$$\text{OH} + (E)\text{-2-hexen-1-ol}$$

where the quoted uncertainties are 2σ from the precision of the least-squares analysis. Uncertainties quoted throughout this paper are at the 2σ (95% confidence interval) level unless stated otherwise.

The temperature dependence of $k_1 - k_4$ is shown in Fig. 4 where the data clearly show that Reactions (R1)–(R4) exhibit a negative temperature dependence. The rate coefficient

Table 2. Summary of experimental conditions and measured rate coefficients, $k_1(T)$, for the OH + (Z)-3-hexen-1-ol reaction.

Temperature (K)	Pressure (Torr, He)	[H₂O₂] (10^{14} molecule cm⁻³)	[OH] (10^{11} molecule cm⁻³)	[(Z)-3-hexen-1-ol] (10^{14} molecule cm⁻³)	Laser Fluence (mJ cm⁻² pulse⁻¹)	$k_1(T)^c$ (10^{-11} cm³ molecule⁻¹ s⁻¹)
244	50	2.0	3.4	0.12–0.69	16.0	14.1 ± 0.1
259	50ᵃ	1.0ᵇ	0.4	0.26–1.2	10.0	13.2 ± 0.3
263	50	1.0	2.3	0.14–1.7	11.4	14.3 ± 0.3
263	50ᵃ	1.0	2.5	0.09–0.75	13.0	14.2 ± 0.3
273	50	0.7	2.5	0.2–1.3	16.0	12.1 ± 0.2
286	50	0.9	2.2	0.10–1.0	12.0	11.3 ± 0.2
296	50	0.46ᵇ	0.2	0.21–1.5	10.0	10.9 ± 0.2
297	50ᵃ	0.46ᵇ	0.2	0.11–1.6	10.0	10.6 ± 0.3
296	50	1.5	4.8	0.11–1.2	16.0	10.6 ± 0.1
297	24	0.9	2.5	0.15–1.2	15.6	10.7 ± 0.2
297	100	0.5	1.6	0.19–1.7	16.0	9.84 ± 0.11
297	50	0.5–2.4	0.5–8.0	0.26–1.6	1.1–16.4	10.7 ± 0.1
309	50ᵃ	1.1	2.8	0.09–1.1	12.5	8.99 ± 0.13
323	50	0.8	2.6	0.23–1.9	16.2	7.78 ± 0.11
348	50ᵃ	0.36ᵇ	0.1	0.27–1.9	9.2	6.49 ± 0.17
374	50	1.0	5.0	0.29–1.0	16.0	6.17 ± 0.09

ᵃ 2 to 5 Torr of O₂ added; ᵇ OH generated by photolysis of HONO at 351 nm. Value given is [HONO]; ᶜ Quoted uncertainties are 2σ from the precision of the least-squares analysis of k' versus [(Z)-3-hexen-1-ol], Eq. (2).

Table 3. Summary of experimental conditions and measured rate coefficients, $k_2(T)$, for the OH + 1-penten-3-ol reaction.

Temperature (K)	Pressure (Torr, He)	[H₂O₂] (10^{14} molecule cm⁻³)	[OH] (10^{11} molecule cm⁻³)	[1-penten-3-ol] (10^{14} molecule cm⁻³)	Laser Fluence (mJ cm⁻² pulse⁻¹)	$k_2(T)^c$ (10^{-11} cm³ molecule⁻¹ s⁻¹)
244	50	0.7	1.4	0.1–3.3	11.8	11.54 ± 0.06
244	20	2.3	3.8	0.2–3.4	10.0	11.87 ± 0.05
244	50ᵃ	1.1	1.6	0.3–5.3	9.1	11.27 ± 0.06
244	50	3ᵇ	1.6	0.1–3.2	21.0	11.12 ± 0.04
271	50	1.1	1.9	0.2–3.8	10.7	8.85 ± 0.07
297	50	0.9	1.9	0.01–4.4	12.3	7.25 ± 0.06
297	20	2.3	1.2	0.3–5.7	3.2	7.28 ± 0.10
297	100	0.4	0.7	0.1–2.07	11.0	7.17 ± 0.04
297	50	0.8	1.4	0.2–1.52	11.1	7.18 ± 0.05
297	50	5.1ᵇ	2.4	0.3–6.5	20.0	6.71 ± 0.04
326	50	1.1	1.7	0.1–3.0	9.4	5.76 ± 0.04
348	50ᵃ	0.6	0.9	0.8–4.76	8.6	4.64 ± 0.19
357	50	1.4	1.6	0.2–6.0	7.0	4.48 ± 0.09
357	50	0.8	1.7	0.2–3.5	12.1	4.82 ± 0.07
373	20	2.6	1.2	0.2–5.6	2.9	3.96 ± 0.09
373	50ᵃ	2.6	4.2	0.3–4.83	9.9	3.97 ± 0.04
374	100	0.8	1.3	0.2–2.4	10.3	4.05 ± 0.02
404	50	2.0	1.4	0.2–5.6	4.1	3.43 ± 0.07
404	50	1.1	2.0	0.3–4.8	11.8	3.55 ± 0.05

ᵃ 2 to 5 Torr of O₂ added; ᵇ OH generated by photolysis of HNO₃ at 248 nm. Value given is [HNO₃]; ᶜ Quoted uncertainties are 2σ from the precision of the least-squares analysis of k' versus [1-penten-3-ol], Eq. (2).

data obey the Arrhenius expression, $k(T) = A\exp(-E/RT)$, over the full range of the temperatures included in this study and a weighted least-squares fit of the data yields (in units of cm³ molecule⁻¹ s⁻¹)

$$k_1(244-374\text{ K}) = (13.3 \pm 0.4) \times 10^{-12} \exp[(580 \pm 10)/T]$$

$$k_2(244-404\text{ K}) = (6.8 \pm 0.22) \times 10^{-12} \exp[(690 \pm 10)/T]$$

$$k_3(243-374\text{ K}) = (6.8 \pm 0.3) \times 10^{-12} \exp[(680 \pm 20)/T]$$

$$k_4(243-376\text{ K}) = (5.4 \pm 0.6) \times 10^{-12} \exp[(690 \pm 20)/T]$$

where the quoted errors are from the precision of the fit. The negative activation energies (E/R) for Reactions (R1)–(R4) are similar with values between −580 and −690 K. The E/R value for the OH + (Z)-3-hexen-1-ol reaction, k_1, of −580 ± 10 K, is ∼15% lower than for the other C5 and C6 unsaturated alcohols included in this study. The negative activation energies observed for these reactions is consistent with a reaction mechanism dominated by the addition of the OH radical to the >C=C< double bond.

Table 4. Summary of experimental conditions and measured rate coefficients, $k_3(T)$, for the OH + (E)-2-penten-1-ol reaction.

Temperature (K)	Pressure (Torr, He)	[H$_2$O$_2$] (10^{14} molecule cm^{-3})	[OH] (10^{11} molecule cm^{-3})	[(E)-2-penten-1-ol] (10^{14} molecule cm^{-3})	Laser Fluence (mJ cm^{-2} pulse^{-1})	$k_3(T)^{\rm c}$ (10^{-11} cm^3 molecule^{-1} s^{-1})
243	50	1.4	0.9	0.13–2.6	3.3	10.94 ± 0.12
243	50$^{\rm a}$	1.8	0.9	0.16–2.36	3.0	11.28 ± 0.14
243	100	0.9	0.8	0.19–1.93	5.0	10.24 ± 0.06
244	50	2.7	1.0	0.12–2.07	2.3	10.50 ± 0.08
271	50$^{\rm a}$	2.6	1.4	0.11–3.77	3.4	9.10 ± 0.10
271	50	1.1	0.5	0.83–2.75	2.7	8.24 ± 0.10
271	50	11.3$^{\rm b}$	0.7	0.13–2.83	3.2	7.87 ± 0.08
271	50	0.9	1.2	0.20–2.82	7.9	8.47 ± 0.11
297	50	3.7	1.5	0.47–5.99	2.5	6.78 ± 0.12
297	50	2.5	1.1	0.13–3.05	2.7	6.97 ± 0.04
297	50	1.9	0.8	0.11–4.34	2.7	6.70 ± 0.06
297	50$^{\rm a}$	2.0	0.7	0.14–2.25	2.3	6.79 ± 0.03
297	100	0.7	0.6	0.24–2.70	5.4	6.40 ± 0.05
297	20	1.9	1.1	0.10–2.93	3.5	6.92 ± 0.07
325	50	1.2	0.5	0.20–3.57	2.4	4.98 ± 0.07
326	50	0.7	1.0	0.14–3.13	8.8	5.37 ± 0.04
326	50	1.2	1.5	0.18–5.99	8.0	5.40 ± 0.07
349	50	1.8	1.1	0.12–3.96	3.8	4.75 ± 0.03
348	50	1.0	1.5	0.21–4.30	8.9	4.74 ± 0.04
374	50	2.8	1.2	0.12–4.97	2.7	4.12 ± 0.03
374	50	2.5	1.1	0.17–4.03	2.6	4.05 ± 0.04
374	100	1.0	0.4	0.15–3.93	2.7	3.89 ± 0.03
373	50	2.3	3.3	0.24–5.33	2.8	3.89 ± 0.07
373	20	2.4	1.2	0.39–3.60	3.1	4.01 ± 0.05
374	50	28.5^{b}	1.6	0.37–3.52	3.0	3.96 ± 0.04

[a] 2 to 5 Torr of O$_2$ added; [b] OH generated by photolysis of HNO$_3$ at 248 nm. Value given is [HNO$_3$]. [c] Quoted uncertainties are 2σ from the precision of the least-squares analysis of k' versus [(E)-2-penten-1-ol], Eq. (2).

Table 5. Summary of experimental conditions and measured rate coefficients, $k_4(T)$, for the OH + (E)-2-hexen-1-ol reaction.

Temperature (K)	Pressure (Torr, He)	[H$_2$O$_2$] (10^{14} molecule cm^{-3})	[OH] (10^{11} molecule cm^{-3})	[(E)-2-hexen-1-ol] (10^{14} molecule cm^{-3})	Laser Fluence (mJ cm^{-2} pulse^{-1})	$k_4(T)^{\rm c}$ (10^{-11} cm^3 molecule^{-1} s^{-1})
243	50	1.3	5.1	0.20–1.2	19.0	9.86 ± 0.06
243	50$^{\rm a}$	1.2	4.3	0.20–1.3	18.0	9.80 ± 0.12
244	100	0.8	2.4	0.34–1.3	14.0	10.3 ± 0.1
258	50	1.6$^{\rm b}$	0.3	0.16–1.3	8.4	8.35 ± 0.39
271	50	0.8	3.2	0.45–2.6	19.0	6.74 ± 0.05
270	100	0.8	2.4	0.20–1.5	14.0	6.72 ± 0.05
296	50	0.6	2.1	0.13–2.1	18.0	5.60 ± 0.19
296	50$^{\rm a}$	0.8	2.8	0.26–2.3	4.6	6.10 ± 0.02
296	50	0.8	2.4	0.12–1.9	14.0	6.24 ± 0.06
296	100	3.0	2.8	0.21–2.1	4.3	6.29 ± 0.11
297	50	1.5	0.5	0.27–2.0	8.4	6.52 ± 0.36
323	100	0.9	0.9	0.15–2.0	4.8	4.78 ± 0.08
348	50	1.1$^{\rm b}$	0.5	0.29–2.2	8.4	3.93 ± 0.22
376	100	1.3	1.2	0.25–2.5	4.8	3.48 ± 0.05
376	20	2.2	3.9	0.16–2.0	8.3	3.46 ± 0.10
376	50	1.9	1.5	0.26–2.2	3.9	3.54 ± 0.07

[a] 2 to 5 Torr of O$_2$ added; [b] OH generated by photolysis of HONO at 351 nm. Value given is [HONO]; [c] Quoted uncertainties are 2σ from the precision of the least-squares analysis of k' versus [(E)-2-hexen-1-ol], Eq. (2).

For the compounds studied here, experiments were performed with and without the addition of O$_2$ to the reaction mixture. Experiments performed with the addition of O$_2$ were intended to scavenge the OH-alcohol adduct as a more stable peroxy, RO$_2$, radical thus minimizing the possible regeneration of OH from the OH-Alcohol adduct formed as a product in Reactions (R1)–(R4). Previous studies of

the analogous OH + 2-methyl-3-buten-2-ol (MBO) reaction have shown that OH regeneration from the OH-MBO adduct dissociation with the release of OH from the alcohol group yields an apparent decrease in the measured rate coefficient in the absence of O$_2$ (Baasandorj and Stevens, 2007; Rudich et al., 1995). The rate coefficients measured in this study with and without added O$_2$ were found to be statistically identical,

Table 6. Summary of rate coefficients for the OH radical reaction with (Z)-3-hexen-1-ol, 1-penten-3-ol, (E)-2-penten-1-ol and (E)-2-hexen-1-ol obtained in this work and taken from the literature.

Compound	Method	$k(298\,\mathrm{K})^{a}$ $(10^{-11}\,\mathrm{cm^{3}\,molecule^{-1}\,s^{-1}})$	A^{a} $(10^{-12}\,\mathrm{cm^{3}\,molecule^{-1}\,s^{-1}})$	E/R^{a} (K)	Reference
(Z)-3-hexen-1-ol	PLP-LIF	10.6 ± 1.2	13 ± 1	-580 ± 10	This work
	RR	10.8 ± 2.2^{b}	–	–	Atkinson et al. (1995)
	PLP-LIF	9.57 ± 2.4^{c}	–	–	Jiménez et al. (2009)
1-penten-3-ol	PLP-LIF	7.12 ± 0.73	6.8 ± 0.7	-690 ± 10	This work
	RR	6.7 ± 0.9^{d}			Orlando et al. (2001)
	PLP-LIF	5.65 ± 0.76^{c}	7.7 ± 0.8^{c}	-606 ± 30^{c}	Jiménez et al. (2009)
(E)-2-penten-1-ol	PLP-LIF	6.76 ± 0.70	6.8 ± 0.8	-680 ± 20	This work
(E)-2-hexen-1-ol	PLP-LIF	6.15 ± 0.75	5.4 ± 0.6	-690 ± 20	This Work

[a] Uncertainties quoted for this work are 2σ including estimated systematic errors; [b] The quoted error is 2σ of the measured rate coefficient ratio (1.67 ± 0.06) combined with a $\pm 20\%$ estimated uncertainty in the rate coefficient of the reference compound, where $k(296\,\mathrm{K}) = 6.48 \times 10^{-11}\,\mathrm{cm^{3}\,molecule^{-1}\,s^{-1}}$ for the OH + (E)-2-butene reference reaction was used; [c] The error is 2σ of the least-squares fit combined with the estimated overall uncertainties; [d] The error is 2σ precision with an estimated 10% uncertainty in the reference rate coefficient where $k(298\,\mathrm{K}) = 2.63 \times 10^{-11}\,\mathrm{cm^{3}\,molecule^{-1}\,s^{-1}}$ for the OH + Propene reference reaction was used. PLP $\equiv$ pulsed laser photolysis – laser induced fluorescence. RR $\equiv$ relative rate.

see Tables 2–5. Therefore, it was concluded that OH regeneration was insignificant, estimated to be <5% for Reactions (R1)–(R4), under the conditions of our measurements. In addition, rate coefficients for the reaction of OD with (Z)-3-hexen-1-ol and (E)-2-hexen-1-ol were also measured. The rate coefficient for the OD + (Z)-3-hexen-1-ol reaction was measured to be $(10.3 \pm 1.1) \times 10^{-11}\,\mathrm{cm^{3}\,molecule^{-1}\,s^{-1}}$ at 50 Torr and 297 K in the absence of O_2, nearly identical to the OH rate coefficient for Reaction (R1). The direct monitoring of OH during the OD reaction also indicated no detectable formation of the OH radical in this system. These results combined with the O_2 independence of k_1 indicate that OH regeneration was negligible in Reaction (R1). Similar behavior was observed for the OD+ (E)-2-hexen-1-ol reaction where the measured rate coefficient at 297 K was $(5.91 \pm 0.57) \times 10^{-11}\,\mathrm{cm^{3}\,molecule^{-1}\,s^{-1}}$.

3.1 Error analysis

The absolute accuracy of the rate coefficients measured for Reactions (R1)–(R4) was dependent on the precision of the measurements, the uncertainties in the determination of the alcohol concentration in the LIF reactor, and the possible contributions of systematic errors to the measurement. The precision of the kinetic measurements was very good and contributed <3% to the overall uncertainty in the measured rate coefficients. The alcohol concentration in the LIF reactor was determined from the measured gas flows as well as the on-line infrared and UV absorption measurements. The agreement between the infrared and UV absorption concentration determinations was better than 5% over the entire range of experimental conditions employed in this study. The UV absorption measurements performed before and after the LIF reactor also agreed to better than 5% under all experimental conditions. This is particularly noteworthy for

the measurements at the temperature extremes and indicates that the reactant alcohol was not lost in the gas flow through the apparatus. The UV and infrared absorption cross sections used in the alcohol concentration determination were measured as part of this work and are estimated to have an uncertainty of <5%.

Systematic uncertainties were primarily evaluated experimentally through the use of a range of experimental conditions during the kinetic measurements including variations in total pressure, buffer gas, photolysis laser fluence, gas flow velocity, initial OH radical concentration, OH precursor, and precursor concentration over the course of the rate coefficient determinations. Measurements were also performed with O_2 added to the reaction mixture to evaluate the influence of possible secondary chemistry of the radicals formed in Reactions (R1)–(R4) on the measured rate coefficients. The measured rate coefficients were found to be independent of the variations in experimental conditions, within the precision of the measurements, as summarized in Tables 2– 5.

The overall 2σ uncertainty in the measured rate coefficients for (Z)-3-hexen-1-ol, 1-penten-3-ol, (E)-2-penten-1-ol, and (E)-2-hexen-1-ol are estimated to be 10, 7, 7 and 8%, respectively. The estimated systematic uncertainties are included in the reported Arrhenius A factors while the uncertainty in the E/R values was taken from the precision of the least-squares fits. The recommended rate coefficients, including total absolute uncertainties, are given in Table 6.

3.2 Comparison with previous studies

Room temperature rate coefficients for Reactions (R1) and (R2) from the literature are included in Table 6 and Fig. 4 for comparison with the results from this work. Atkinson et al. (1995) measured the rate coefficient for the OH + (Z)-3-hexen-1-ol reaction,
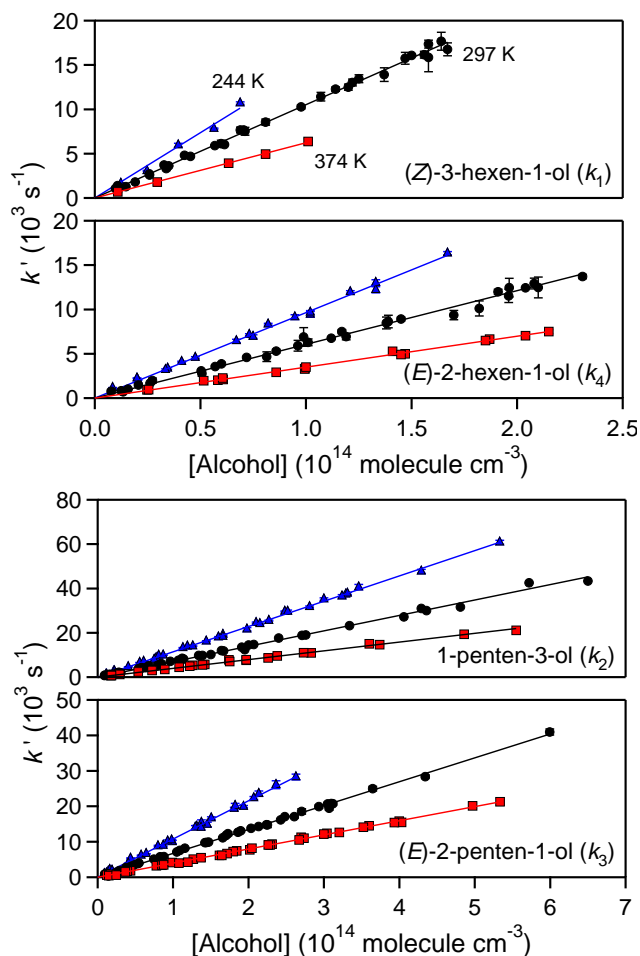
Fig. 3. Pseudo-first-order rate coefficient, k', data plotted versus the unsaturated alcohol concentration for (Z)-3-hexen-1-ol $((Z)$-$CH_3CH_2CH=CHCH_2CH_2OH)$ (k_1), (E)-2-hexen-1-ol $((E)$-$CH_3CH_2CH_2CH=CHCH_2OH)$ (k_4), 1-penten-3-ol $(CH_3CH_2CH(OH)CH=CH_2)$ (k_2), (E)-2-penten-1-ol $((E)$-$CH_3CH_2CH=CHCH_2OH)$ (k_3) at 244 K ($\triangle$), 297 K ($\bigcirc$), and 374 K ($\square$). The error bars are the 2σ uncertainties from the fits to the individual OH decays (e.g. the data shown in Fig. 1). The lines are the least-squares fits of the data to Eq. (2) and the slope yields the bimolecular rate coefficient k.
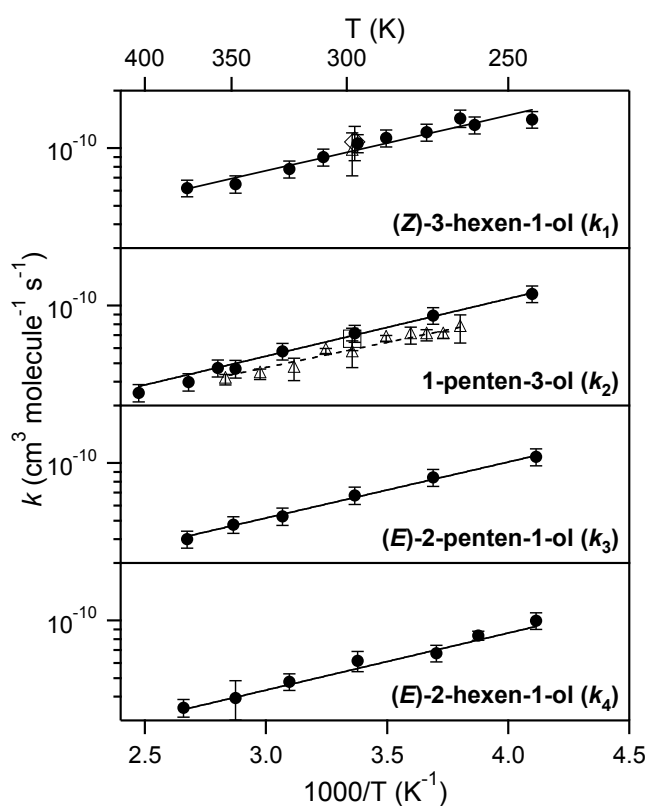

Fig. 4. Temperature dependent rate coefficient data for Reactions (R1)–(R4), Arrhenius plot, from this work ($\bullet$). The error bars are the 2σ uncertainty including estimated systematic errors. The lines are least-squares fits of the data to the Arrhenius expression, $\ln(k) = \ln(A)-E/RT$ where the results are given in Table 6. For comparison, results from previous studies, as described in the text, are included: $OH + (Z)$-3-hexen-1-ol at room temperature by Atkinson et al. (1995) ($\diamond$) and Jiménez et al. (2009) ($\triangle$); $OH + $1-penten-3-ol at room temperature by Orlando et al. (2001) ($\square$) and between 263 and 353 K by Jiménez et al. (2009) ($\triangle$). The results from the previous studies are also included in Table 6.

k_1, using a relative rate method. They reported $k_1(298\,\mathrm{K}) = (10.8 \pm 2.2) \times 10^{-11}\,\mathrm{cm^3\,molecule^{-1}\,s^{-1}}$, which is in excellent agreement with the value obtained in the present study. Jiménez et al. (2009) reported $k_1(298\,\mathrm{K}) = (9.57 \pm 2.42) \times 10^{-11}\,\mathrm{cm^3\,molecule^{-1}\,s^{-1}}$ obtained using a PLP-LIF technique, which was very similar to the method used in the present study. Although the reported rate coefficient is slightly less than obtained in our work the agreement is within the combined uncertainties of the measurements.

Orlando et al. (2001) used a relative rate method to determine $k_2(298\,\mathrm{K}) = (6.7 \pm 0.9) \times 10^{-11}\,\mathrm{cm^3\,molecule^{-1}\,s^{-1}}$ in

good agreement with the value determined in our work. As shown in Fig. 5, the rate coefficient data reported by Jiménez et al. (2009) for Reaction (R2) over the temperature range 263–353 K is systematically less, by $\sim$25 %, than measured in our work. The temperature dependence of k_2 obtained in the two studies is in reasonable agreement, $E/R = -690 \pm 20$ K in our work compared with $E/R = -606 \pm 30$ K reported by Jiménez et al. The difference between the rate coefficients is reduced to $\sim$15 % when the rate coefficient data are normalized to the same 185 nm absorption cross section for 1-penten-3-ol, see Table 1; absorption measurements at 185 nm were used in both studies to measure the 1-penten-3-ol concentration.

The room temperature rate coefficients for the reaction of OH with (E)-2-penten-1-ol and (E)-2-hexen-1-ol can be compared with the values predicted using the

structure activity relationships (SAR) of Kwok and Atkinson (1995) combined with updated enhancement factors for the $-CH_2OH$ and $-CH_2CH_2OH$ groups from the work of Papagni et al. (2001). The SAR estimated rate coefficients for Reactions (R3) and (R4) are identical since the reactivity factors for C_2H_5 and C_3H_7 are the same. The SAR estimated rate coefficient is 1.33×10^{-10} cm^3 molecule^{-1} s^{-1}, which is approximately twice the experimentally measured values of $(6.76 \pm 0.70) \times 10^{-11}$ cm^3 molecule^{-1} s^{-1} and $(6.15 \pm 0.75) \times 10^{-11}$ cm^3 molecule^{-1} s^{-1}. Note that the rate coefficient measured in our work for the shorter chain length molecule is actually greater. The level of agreement between the SAR estimate and the experimental values is probably within the acceptable range for the SAR estimation method. The SAR rate coefficient for the $OH + (Z)$-3-hexen-1-ol reaction is in good agreement with the experimental value, to better than 10%, while the SAR rate coefficient for the 1-penten-3-ol reaction is only ~15% less than the experimental value. The difference between the estimated and measured rate coefficients for the (E)-2-penten-1-ol and (E)-2-hexen-1-ol reactions may in part be due to the steric hindrance in the OH addition to the *trans* isomers, which may not be adequately accounted for in the SAR reactivity coefficients. We mention this because the measured rate coefficient for the $OH + (Z)$-2-penten-1-ol (Orlando et al., 2001) reaction, which should have less steric hindrance, is $(1.06 \pm 0.15) \times 10^{-10}$ cm^3 molecule^{-1} s^{-1} in agreement with the SAR value of 9.0×10^{-11} cm^3 molecule^{-1} s^{-1}. The steric effect seems to offset the enhancement associated with the presence of the $-CH_2OH$ group adjacent to the double bond.

It is also worthwhile to compare the rate coefficients for the C5 compounds included in this study with that for the OH reaction with $(CH_3)_2C(OH)CH = CH_2$ (2-methyl-3-buten-2-ol, MBO) which has a similar molecular structure. MBO is a C5 unsaturated alcohol commonly found in remote forests and has been studied in the laboratory by several groups (Baasandorj and Stevens, 2007; Imamura et al., 2004; Rudich et al., 1995). Room temperature rate coefficients for the $OH + MBO$ reaction have been reported in the range $(5.8–6.6) \times 10^{-11}$ cm^3 molecule^{-1} s^{-1} in the presence of O_2. The absolute rate coefficient measurements for the $OH + MBO$ reaction are complicated somewhat by the regeneration of OH radicals from the elimination of the alcohol OH group from the OH-MBO adduct, which was found (as described earlier) not to be a problem for the C5 compounds in the present study. Overall the rate coefficients for the C5 compounds studied in this work are very similar to that for the MBO reaction. The temperature dependence of the rate coefficients studied here are also similar to that of the $OH + MBO$ reaction; Rudich et al. (1995) reported $E/R = (-610 \pm 50)$ K.

In general, the rate coefficients for the $OH +$ unsaturated alcohol reactions are only weakly dependent on the chain length of the alcohol. The room temperature rate coefficients for 1-penten-3-ol, (E)-2-penten-1-ol, and (E)-2-hexen-

1-ol range between 6.15×10^{-11} cm^3 molecule^{-1} s^{-1} and 7.12×10^{-11} cm^3 molecule^{-1} s^{-1}. Papagni et al. (2001) measured reaction rate coefficients for a series of C3 to C5 unsaturated alcohols. Their measured rate coefficient for MBO was similar to the rate coefficients for allyl alcohol ($CH_2 = CHCH_2OH$) $(5.46 \pm 0.35) \times 10^{-11}$ cm^3 molecule^{-1} s^{-1}, 3-buten-1-ol ($CH_2 = CHCH_2CH_2OH$) $(5.50 \pm 0.20) \times 10^{-11}$ cm^3 molecule^{-1} s^{-1}, and 3-buten-2-ol ($CH_2 = CHCH(OH)CH_2$) $(5.93 \pm 0.23) \times 10^{-11}$ cm^3 molecule^{-1} s^{-1}. This data set suggests that the rate coefficient is also only weakly dependent on the position of the carbon-carbon double bond with respect to the position of the alcohol group. The (E)-/(Z)- geometry of the compound seems to play a more important role in determining the compounds reactivity. For the compounds with (E)- or *trans* functional groups around the carbon-carbon double bond a rate coefficient in the range $(6–7) \times 10^{-11}$ cm^3 molecule^{-1} s^{-1} with $E/R \approx -680$ K was observed. When the functional groups are (Z)- or *cis* there appears to be less steric hindrance leading to higher reactivity and a less negative activation energy, $E/R \approx -580$ K. The rate coefficients for the (Z)- or *cis* isomer were found to be a factor of ~1.6 greater than for the (E)- or *trans* isomer.

4 Conclusions

Gas-phase rate coefficients for the reaction of several atmospherically relevant unsaturated alcohols with the OH radical were measured as a function of temperature (243–404 K). The rate coefficients show a negative temperature dependence that is consistent with a reaction mechanism involving the addition of OH to the carbon-carbon double bond. No pressure dependence was observed over the pressure range 20–100 Torr (He) indicating that these reactions are in the high-pressure limit for the temperatures and pressures included in this study. Unsaturated compounds are expected a priori to have short atmospheric lifetimes due to their high gas-phase reactivity with the OH radical. The BVOCs included in this study have estimated lifetimes due to loss by reaction with the OH radical of several hours (about 2.5 to 5 h for an OH concentration of 1×10^6 molecule cm^{-3}). In this study, differences in reactivity between (E)- and (Z)- geometrical isomers were observed with the (Z)- isomers exhibiting greater reactivity, which is not accounted for quantitatively in the Kwok and Atkinson (1995) structure activity relationship. The rapid oxidation and degradation product formation of the unsaturated compounds included in this study need to be accounted for in air quality models on local and regional scales. The rate coefficients measured in this work are appropriate for use in atmospheric models.

References

Alvarado, A., Tuazon, E. C., Aschmann, S. M., Arey, J., and Atkinson, R.: Products and mechanisms of the gas-phase reactions of OH radicals and O_3 with 2-methyl-3-buten-2-ol, Atmos. Environ., 33, 2893–2905, 1999.

Arey, J., Winer, A. M., Atkinson, R., Aschmann, S. M., Long, W. D., and Morrison, C. L.: The emission of (*Z*)-3-hexen-1-ol, (*Z*)-3-hexenylacetate and other oxygenated hydrocarbons from agricultural plant-species, Atmos. Environ., 25, 1063–1075, 1991.

Aschmann, S. M., Shu, Y. H., Arey, J., and Atkinson, R.: Products of the gas-phase reactions of cis-3-hexen-1-ol with OH radicals and O_3, Atmos. Environ., 31, 3551–3560, 1997.

Atkinson, R., Arey, J., Aschmann, S. M., Corchnoy, S. B., and Shu, Y. H.: Rate constants for the gas-phase reactions of cis-3-hexen-1-ol, cis-3-hexenylacetate, trans-2-hexenal, and linalool with OH and NO_3 radicals and O_3 at 296 ± 2 K, and OH radical formation yields from the O_3 reactions, Int. J. Chem. Kinet., 27, 941–955, 1995.

Baasandorj, M. and Stevens, P. S.: Experimental and theoretical studies of the kinetics of the reactions of OH and OD with 2-methyl-3-buten-2-ol between 300 and 415 K at low pressure, J. Phys. Chem. A, 111, 640–649, 2007.

Baker, J., Arey, J., and Atkinson, R.: Rate constants for the gas-phase reactions of OH radicals with a series of hydroxyaldehydes at 296 ± 2 K, J. Phys. Chem. A, 108, 7032–7037, 2004.

Davis, M. E., Gilles, M. K., Ravishankara, A. R., and Burkholder, J. B.: Rate coefficients for the reaction of OH with (*E*)-2-pentenal, (*E*)-2-hexenal, and (*E*)-2-heptenal, Phys. Chem. Chem. Phys., 9, 2240–2248, 2007.

Ebel, R. C., Mattheis, J. P., and Buchanan, D. A.: Drought stress of apple-trees alters leaf emissions of volatile compounds, Physiol. Plantarum., 93, 709–712, 1995.

Fisher, A. J., Grimes, H. D., and Fall, R.: The biochemical origin of pentenol emissions from wounded leaves, Phytochemistry, 62, 159–163, 2003.

Grosjean, E. and Grosjean, D.: The gas phase reaction of unsaturated oxygenates with ozone: Carbonyl products and comparison with the alkene-ozone reaction, J. Atmos. Chem., 27, 271–289, 1997.

Guenther, A., Geron, C., Pierce, T., Lamb, B., Harley, P., and Fall, R.: Natural emissions of non-methane volatile organic compounds; carbon monoxide, and oxides of nitrogen from North America, Atmos. Environ., 34, 2205–2230, 2000.

Guenther, A., Hewitt, C. N., Erickson, D., Fall, R., Geron, C., Graedel, T., Harley, P., Klinger, L., Lerdau, M., McKay, W. A.,

Pierce, T., Scholes, B., Steinbrecher, R., Tallamraju, R., Taylor, J., and Zimmerman, P.: A global-model of natural volatile organic-compound emissions, J. Geophys. Res. Atmos., 100, 8873–8892, 1995.

Hatanaka, A. and Harada, T.: Leaf-alcohol formation of cis-3-hexenal, trans-2-hexenal and cis-3-hexenol in macerated thea-sinensis leaves, Phytochemistry, 12, 2341–2346, 1973.

Heiden, A. C., Kobel, K., Langebartels, C., Schuh-Thomas, G., and Wildt, J.: Emissions of oxygenated volatile organic compounds from plants – part I: Emissions from lipoxygenase activity, J. Atmos. Chem., 45, 143–172, 2003.

Imamura, T., Iida, Y., Obi, K., Nagatani, I., Nakagawa, K., Patroescu-Klotz, J., and Hatakeyama, S.: Rate coefficients for the gas-phase reactions of OH radicals with methylbutenols at 298 K, Int. J. Chem. Kinet., 36, 379–385, 2004.

Jiménez, E., Lanza, B., Antiñolo, M., and Albaladejo, J.: Photooxidation of leaf-wound oxygenated compounds, 1-penten-3-ol, (*Z*)-3-hexen-1-ol, and 1-penten-3-one, initiated by OH radicals and sunlight, Environ. Sci. Technol., 43, 1831–1837, 2009.

Karl, T., Fall, R., Jordan, A., and Lindinger, W.: On-line analysis of reactive VOCs from urban lawn mowing, Environ. Sci. Technol., 35, 2926–2931, 2001.

Kirstine, W., Galbally, I., Ye, Y. R., and Hooper, M.: Emissions of volatile organic compounds (primarily oxygenated species) from pasture, J. Geophys. Res. Atmos., 103, 10605–10619, 1998.

Kwok, E. S. C. and Atkinson, R.: Estimation of hydroxyl radical reaction-rate constants for gas-phase organic-compounds using a structure-reactivity relationship – an update, Atmos. Environ., 29, 1685–1695, 1995.

Nakamura, S. and Hatanaka, A.: Green-leaf-derived C6-aroma compounds with potent antibacterial action that act on both gram-negative and gram-positive bacteria, J. Agricult. Food Chem., 50, 7639–7644, 2002.

Noda, J., Hallquist, M., Langer, S., and Ljungstrom, E.: Products from the gas-phase reaction of some unsaturated alcohols with nitrate radicals, Phys. Chem. Chem. Phys., 2, 2555–2564, 2000.

Noda, J., Nyman, G., and Langer, S.: Kinetics of the gas-phase reaction of some unsaturated alcohols with the nitrate radical, J. Phys. Chem. A, 106, 945–951, 2002.

Orlando, J. J., Tyndall, G. S., and Ceazan, N.: Rate coefficients and product yields from reaction of OH with 1-penten-3-ol, (*Z*)-2-penten-1-ol, and allyl alcohol (2-propen-1-ol), J. Phys. Chem. A, 105, 3564–3569, 2001.

Papagni, C., Arey, J., and Atkinson, R.: Rate constants for the gas-phase reactions of OH radicals with a series of unsaturated alcohols, Int. J. Chem. Kinet., 33, 142–147, 2001.

Pfrang, C., Martin, R. S., Canosa-Mas, C. E., and Wayne, R. P.: Gas-phase reactions of NO_3 and N_2O_5 with (*Z*)-hex-4-en-1-ol, (*Z*)-hex-3-en-1-ol ("leaf alcohol"), (*E*)-hex-3-en-1-ol, (*Z*)-hex-2-en-1-ol and (*E*)-hex-2-en-1-ol, Phys. Chem. Chem. Phys., 8, 354–363, 2006.

Pfrang, C., Romero, M. T. B., Cabanas, B., Canosa-Mas, C. E., Villanueva, F., and Wayne, R. P.: Night-time tropospheric chemistry of the unsaturated alcohols (*Z*)-pent-2-en-1-ol and pent-1-en-3-ol: Kinetic studies of reactions of NO_3 and N_2O_5 with stress-induced plant emissions, Atmos. Environ., 41, 1652–1662, 2007.

Rudich, Y., Talukdar, R., Burkholder, J. B., and Ravishankara, A. R.: Reaction of methylbutenol with hydroxyl radical – Mechanism and atmospheric implications, J. Phys. Chem., 99, 12188–

12194, 1995.

Sander, S. P., Golden, D. M., Kurylo, M. J., Huie, R. E., Orkin, V. L., Moortgat, G. K., Ravishankara, A. R., Kolb, C. E., Molina, M. J., Finlayson-Pitts, B. J., and Wine, P. H.: Chemical Kinetics and Photochemical Data for Use in Atmospheric Studies, Evaluation Number 15, JPL Publication 06–2, Jet Propulsion Laboratory, California Institute of Technology, 2006.

Upadhyaya, H. P., Kumar, A., Naik, P. D., Sapre, A. V., and Mittal, J. P.: Kinetics of OH radical reaction with allyl alcohol ($H_2C = CHCH_2OH$) and propargyl alcohol ($HC \equiv CCH_2OH$) studied by LIF, Chem. Phys. Lett., 349, 279–285, 2001.

Vaghjiani, G. L. and Ravishankara, A. R.: Kinetics and mechanism of OH Reaction with CH_3OOH, J. Phys. Chem., 93, 1948–1959, 1989.